Incremental Capacity Analysis on Module level Li-ion Batteries for Echelon Utilization

Chris de Jong - 1 July 2022
Supervisors: S.Azizighalehsari, P Venugopal
BSc. Thesis Electrical Engineering
University of Twente, Enschede, The Netherlands
Department of Electrical Engineering, Mathematics and Computer Science

***Abstract* - Degradation of lithium-ion batteries (LIBs) is a complex process which expresses itself as capacity and power fade. Sophisticated analysis techniques are required to provide insight into the internal battery chemistry and its state of health (SOH). Incremental capacity analysis (ICA) is a battery analysis method which can provide this insight and determine the SOH. This paper deals with incremental capacity (IC) curves analyzing LIB modules with two different chemistries. The influence of each individual cell on the IC curve of the module and also the influence of the discharge current on IC curves have been considered. The evolution of IC curves as the battery cell/module gets aged is investigated. Finally, a comparison between several modules is given based on their ICA.**

***Key Terms* - cell level, electric vehicles, incremental capacity analysis, lithium-ion batteries, module level, state of health.**

I. Introduction

The last couple of decades has shown a revolution of lithium-ion battery (LIB) technology. The price per kWh dropped from over $7,500 in 1991 to less than $200 in 2018, a reduction of around 97% [1]. LIBs have become the go-to energy storage medium for all kinds of small electric devices such as mobile phones, RC vehicles, etc. LIBs, due to their exceptional properties and fast-growing technology, are the most favourable batteries to be used in electric vehicles (EVs). The global EV stock has risen from 2000 EVs to over 7 million EVS on the roads in 2019 [2]. A major downside of LIBs is that they degrade during operation. Internal battery chemistry starts to change as LIBs experience charge-discharge cycles. These unwanted chemical changes inside the battery cause decrease in performance and capacity [3]. Degradation is especially detrimental in EVs since the batteries operate under high-performance conditions under harsh environments and all capacity lost becomes dead weight which the vehicle has to move around. In general, when LIB packs in EVs lose over 20% of their original capacity they are replaced. The current way to dispose of these LIBs is to recycle them for their raw materials, which is energy-intensive [4]. A more efficient solution would be echelon utilization. Echelon utilization is the reusing degraded LIBs directly in applications that are less sensitive to capacity or power fade of the battery. Examples of such applications are mostly stationary energy storage systems such as powerwalls and large energy storage for renewable energy sources [5].

LIB degradation is a complex process and it can be difficult to determine the quality of the cell based on a single parameter such as capacity fade. There are many LIB degradation mechanisms that affect battery performance. A reliable way to estimate the state of health (SOH) of LIBs is the key to determining the remaining useful life (RUL) and overall cell quality. The SOH of a LIB can also indicate if the cells are still safe to use since LIBs can catch fire or explode under certain conditions [6]. There are many methods to measure and estimate the SOH of LIBs. They can be categorised into two main groups *in situ* (measuring during operation) and *postmortem* (measuring after salvaging).

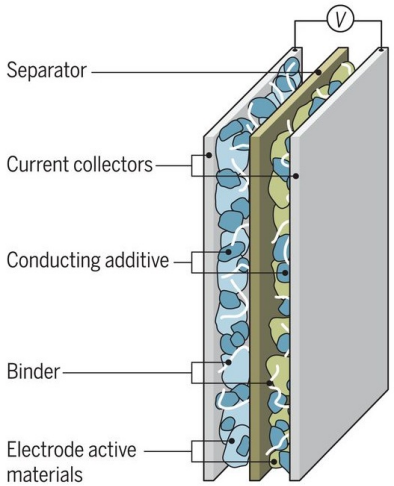

Fig. 1: Internal battery structure of LIB [3].

A. LIB Degradation Mechanisms

The most notable effect of LIB degradation mechanisms is capacity and power fade [3]. These are the effects that the user of the LIB experiences and can indicate whether a LIB is suited for a certain application. However, these effects provide little insight into the SOH of the battery. Capacity and power fade are caused by multiple complex underlying degradation mechanisms. These underlying degradation mechanisms are

hard to measure and individually do not cause direct observable effects on battery performance [7]. The most common and significant effects of degradation mechanisms are loss of lithium inventory (LLI), loss of active material (LAM), ohmic resistance increase (ORI), and lithium plating [7]. Fig. 1 shows a basic model of a LIB. All components inside LIBs are prone to ageing and degrade in different manners with differing effects on the battery performance.

The biggest contributor to the ageing of LIBs is the buildup of the solid electrolyte interphase (SEI) buildup [7]. An SEI layer is a thin layer on the anode of LIBs that is generated during its lifetime. Having an SEI layer inside LIBs is not necessarily a disadvantage. On the contrary, a proper SEI layer inside LIBs significantly extends their lifetime and makes LIBs rechargeable [8]. The SEI is generated on the anode during the first few charge-discharge cycles. This SEI layer passivates the electrode surface and thus prevents electron transport between the electrode and the electrolyte. Lithium ions on the other hand are allowed to pass through the SEI otherwise no reaction could take place to produce electrical energy. These properties of the SEI protect the LIB from electrolyte reacting with the electrode. This reaction causes electrolyte reduction and electrode corrosion which enhances LLI and ORI [7, 8]. SEI formation is most prominent during the first few cycles but does not cease after many cycles. Lithium ions are consumed during the reaction that creates the SEI layer and thus enhances LLI. The formation of SEI also releases gases which leads to LAM and enhances electrode degradation in general [7, 9]. A thicker SEI layer decreases the lithium ion transport which enhances ORI. At a high number of cycles, the SEI layer may propagate into the electrode and become more porous [7, 8]. The decrease in active surface area of the electrode caused by the penetration of SEI into the electrode causes further ORI. The increase in porosity causes electrolyte to come into contact and react with the electrode which causes electrolyte decomposition and enhances LLI and ORI [7]. SEI formation is accelerated by operation in high-temperature environments and prolonged idling at a high state of charge (SOC) [7]. It is thus important for LIBs that the SEI layer stays at its optimum thickness for the majority of its lifetime so that it prevents electrolyte decomposition but does not impede ionic transport or degrade the electrode.

Lithium plating is another degradation mechanism that has a high impact on the performance of LIBs. Lithium plating is the buildup of metallic lithium on the anode. Lithium plating occurs when the anode voltage drops below 0V which most often happens during charging [10]. This formation of lithium consumes lithium ions and thus enhances LLI. Lithium plating also enhances ORI which in turn accelerates lithium plating, it is a self-accelerating process [11]. SEI formation is also accelerated by lithium plating since the metallic lithium can react with the electrolyte which creates SEI compounds [10]. The major problem with lithium plating is the safety issues that arise when lithium plating has occurred. Lithium dendrites caused by lithium plating can cause short circuits by penetrating the separator [11]. The reaction between metallic lithium and the electrolyte is fast and exothermic which can cause thermal runaway and make the LIB catch fire or explode [11]. Especially when flakes of metallic lithium lose contact with the anode and are fully surrounded by electrolyte this reaction is accelerated. Lithium plating is accelerated by high charging currents, low-temperature environments, and prolonged storage at high SOC [7].

B. Battery Analysis Methods

There are many methods available for analysing LIBs and estimating the SOH. This paper discusses ICA which is a non-invasive method that can be used for both *in situ* and *postmortem* analysis. More novel battery analysis methods that rely on impedance measurements such as electrochemical impedance spectroscopy (EIS) and nonlinear frequency response analysis (NFRA) are becoming more popular. These methods rely on impedance measurements across the frequency spectrum [12, 13]. These methods are mostly used in *postmortem* analysis because they require high sinusoidal currents during testing. EIS is usually performed using a sinusoidal input current with an amplitude of 0.15C and NFRA requires at least 1.5C input amplitude [12, 13]. ICA is more suited for *in situ* measurements since it does not require special current waveforms or high frequency measurements. NFRA was also considered for this paper but the current requirements restricted the possible LIBs to analyze to small pouch cells unsuited for EV applications.

C. Incremental Capacity Analysis

More primitive techniques for analyzing battery health are only able to measure capacity and internal resistance. These parameters give rough estimates of how much the LIB has aged but provide little insight into the internal chemistry of the LIB. The voltage curve of LIBs during charging and discharging is rich with information about the LIB. The electrode material determines the potential range and voltage plateaus [14]. As stated before the main contributors to LIB ageing are changes in the electrode material such as SEI formation and lithium plating. These changes in the electrode chemistry also change the potential range and voltage plateaus during charging and [14]. These effects that the electrode material has on the charging and discharging voltage can be measured quite easily but hard to analyze. The problem with voltage curves is that the flat plateaus are hard to distinguish from each other and may even overlap. In voltage curves, it is not immediately visible with the naked eye how many different regions are present and where they are located which makes it hard to analyze. ICA is a method that analyzes the change in voltage and the corresponding change in capacity of LIBs [15]. Voltage plateaus during constant-current (CC) charging or discharging correspond to large amounts of energy being added to the LIBs and slopes correspond to low amounts of energy being added. This means that during voltage plateaus every constant voltage increment results in large increments in capacity and slopes result in low increments in capacity. The incremental capacity (IC) is the ratio between a change in voltage ΔV and a change in capacity ΔQ. An example of how voltage plateaus and slopes affect the IC values can be seen in Fig. 2.

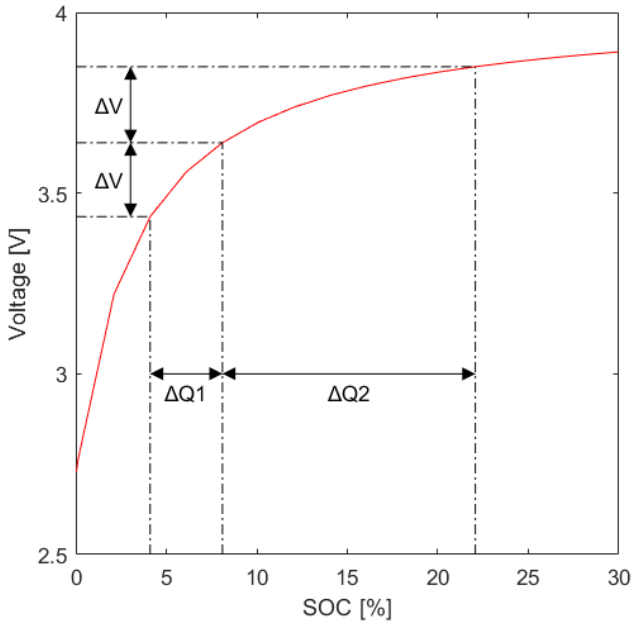

Fig. 2: Example of how the voltage curve shape affects the IC.

A good way to analyze LIBs is to examine the IC values in relation to the battery voltage. This can be done by taking the derivative of Q-V curves with respect to V. However, since voltage measurements and thus Q-V curves are discrete and not continuous IC curves have to be approximated. This approximation is done by simply dividing the change in capacity ΔQ by the constant voltage increment ΔV. Equation 1 describes how for a constant voltage increment the IC is calculated [16].

$$IC_n = \frac{\Delta Q_n}{\Delta V} \tag{1}$$

The IC curves that are obtained using this technique are rich with information about the SOH of the LIB. IC curves have distinct peaks that uniquely respond to changes in battery chemistry. IC peaks can be used to accurately estimate the SOH and require little computing power to do so since the curves contain lots of information [17]. For this reason ICA is a good option where an *in situ* technique is required [18]. Low computational power requirements makes ICA easily implementable in battery management systems (BMSs). ICA can be performed during constant-current-constant-voltage (CCCV) charging and during discharging in operation. When measuring the IC curves of LIBs during operation it is easy to track the SOH during its lifetime. Using ICA as a *postmortem* technique is also possible but without a proper model or reference to measurements of unaged LIBs, only rough SOH estimations can be made.

D. Effect of degradation mechanisms on IC curves

Since the IC curve is the derivative of the capacity with respect to the voltage the area underneath the IC curve must be the total capacity. This is expressed mathematically in Equation 2.

$$Q_{total} = \int_{v_{min}}^{v_{max}} \frac{dQ}{dv} dv \tag{2}$$

Every type of LIB chemistry will have a different characteristic IC curve with different peaks and a different evolution. However, since capacity fade is always present in aged cells in general a decrease in the magnitude of IC peaks is expected. The important information in IC curves is the change of the peaks and valleys. A typical voltage curve during CC discharging can be seen in Fig. 3.

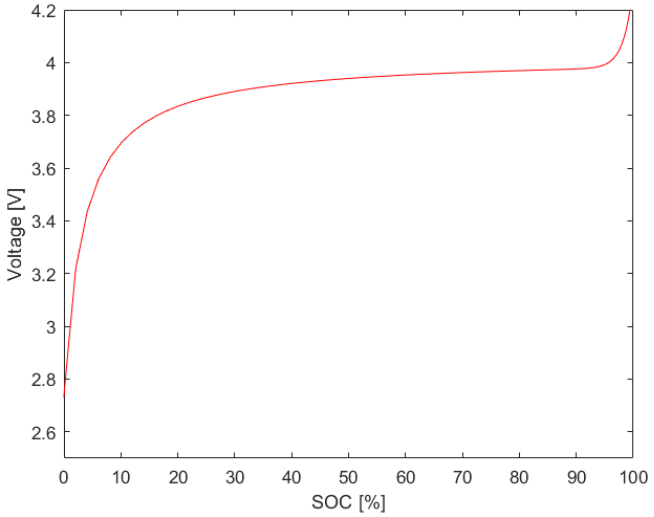

Fig. 3: Voltage curve of LIB during CC discharge.

It is expected that at low and high voltages the IC curve is close to zero and that IC peaks occur at voltages in between. An example of how different degradation mechanisms affect the IC curve of a lithium iron phosphate (LFP) battery with a graphite anode can be seen in Fig. 4. There are three peaks that can be distinguished that react to degradation inside the LIB. These peaks will be referred to as peaks 1, 2, and 3 with peak 1 corresponding to the rightmost peak, peak 2 corresponding to the middle peak, and peak 3 corresponding to the leftmost peak. As stated before the four main degradation mechanisms are LLI, LAM, ORI, and lithium plating. LAM can be categorized into LAM at the anode (LAM_{NE}) and LAM at the cathode (LAM_{PE}).

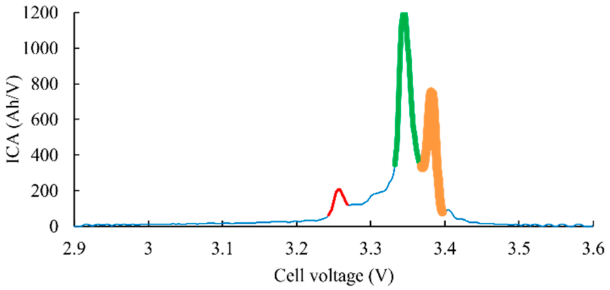

Fig. 4: IC curve of LFP with graphite anode [19].

The formation of SEI is the biggest contributor to LLI. The formation of SEI reduces the number of lithium ions that can react to create power. This causes the voltage plateau of the SEI to shift to higher SOCs and lose capacity [18, 20]. This shifting and the general capacity decrease causes a decrease in the area and magnitude of peak 1. The voltage plateau can eventually shift out of the voltage range of the LIB which causes a further reduction of peak 1. When peak 1 is almost fully extinct, peak 2 starts to decrease [18]. The magnitude and area of peak 3 are unaffected by LLI but its position also shifts to higher SOCs and thus shifts to the right [18]. In general, LLI shifts peak 3 to the right and causes a decrease in peak 1 and only a decrease in peak 2 after peak 1 has been depleted.

LAM_{NE} does not result in any voltage plateaus shifting. LAM_{NE} leaves the characteristics of each process intact [20]. However, since there is less active material to react with the lithium ions the overall capacity decreases. Therefore, LAM_{NE} causes a decrease across the entire IC curve.

Commonly, the anode of LFP batteries is the electrode that limits the capacity [20]. This causes LAM_{PE} to have little to no effect on the IC curve. Only when the cathode becomes the electrode that limits the capacity will it cause peak 1 to decrease.

Since ORI does not result in capacity fade the area of the peaks is unaffected. ORI does shift the entire IC curve to higher voltages. The shape of the IC curve can change due to ORI because the shift to higher voltages is not necessarily symmetrical [20].

Lithium plating is accompanied by LLI and ORI so the same effects that LLI and ORI have on the IC curve can also be expected when lithium plating is present. Lithium plating can also cause a new peak to develop in the higher voltage range [18].

Degradation mechanisms across different battery chemistries mostly have the same effect. Characteristics peaks either decrease or shift position and new peaks arise when lithium plating is present [21].

II. Methodology

ICA was performed on two types of cells. Prismatic lithium manganese oxide (LMO) and cylindrical nickel manganese cobalt (NMC) cells. The investigated LMO cells are retired LIBS from an EV application whose historical performance data is unknown. Four modules consisting of 8 LMO in series were available. Two modules of NMC cells were investigated. One module containing unaged cells and one module containing aged cells of which the historical performance data is also unknown. Both NMC modules consist of 6 cells in series. The specifications according to the datasheet of the cells can be found in Table I.

TABLE I: Specifications of investigated cells.

Battery chemistry	LMO	NMC
Capacity [Ah]	40Ah	2.7Ah
Nominal voltage [V]	3.65V	3.6V
Voltage range [V]	2.65V-4.0V	2.5V-4.2V
Cathode material	Lithium manganese oxide	LiNiMnCoO2
Anode material	Carbon	Carbon

The following topics of interest were measured:

- Influence of discharge current on IC curves
- Influence of individual cells on module IC curve
- Differences between IC curves of new and old modules

Only discharge IC curves are evaluated in this study. ICA can also be performed during charging and should produce characteristic IC curves. However, during the CV stage of charging LIBs it is more complex to compute the difference in capacity for fixed voltage steps. Since the CV stage occupies a large portion of the charging process IC curves produced during discharging was opted for. It is possible to extract useful information from the CV curves as shown by Wang *et al*. [22].

A. Measurement Setup

To generate the IC curves the batteries have to be discharged with a constant current. This was done using the Chroma 6314A DC electronic load mainframe with 4 Chroma 63103A load modules. Each module is capable of sinking up to 60A at a maximum power of 300W [23]. 4-point voltage and current measurements were performed during discharging using the electronic load. Load modules were connected in parallel when more than 300W was required. During measurements, individual cells were monitored manually using a multimeter. When one of the cells dropped below the cut-off voltage, measurements were terminated to prevent deep discharging of the LIBs. The cut-off voltage of the LMO cells was set to 3V and the cut-off voltage of the NMC cells was set to 2.5V. All measurements were performed in a climate-controlled room kept at 23C°. After measurements, the LIBs were charged using bench power supplies while again monitoring individual cells manually using a multimeter. A schematic of the measurement setup for a single load module can be seen in Fig. 5.

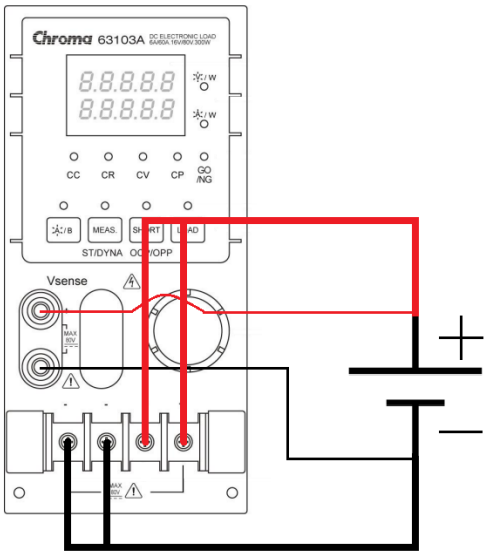

Fig. 5: Schematic of measurement setup for single load module (original drawing of load module from manual [23]).

B. Data processing

The Chroma electronic load provides voltage and capacity measurements in the form of a .txt document. MATLAB is able to import these documents and analyze the results. A simple for loop which computes the IC when the voltage changes value was used to compute IC curves. This MATLAB code can be found in the appendix. Voltage and capacity measurements have discrete values and very small voltage decrements are analyzed. This makes the output jumpy and susceptible to measurement noise. A Gaussian filter is effective in filtering out high-frequency noise from a desired low-frequency signal [24]. This makes it effective for filtering IC curves since the desired signal changes slowly while the noise that is present is in the same order of magnitude as the sampling frequency. The equation for a Gaussian filter can be seen in Equation 3.

$$G(x) = \frac{1}{\sigma\sqrt{2\pi}} e^{\frac{-(x-\mu^2}{2\sigma^2}} \tag{3}$$

Where σ is the standard deviation of the filter and μ is the mean value.

III. Results and Discussion

A. Gaussian Filter

As stated before IC peaks can be hard to distinguish from the raw IC curve. The values for μ and σ have to be determined. μ is generally set to a small number and has a default value of 0 in MATLABs `imgaussfilt()` function. A too low value for σ does not filter the noise enough and leaves the output with noticeable noise still present. Too high values for σ result in information being lost during filtering. The Gaussian filter was implemented in MATLAB with the default value of 0 for μ and a value of 5 for σ for LMO LIBs and a value of 10 for NMC LIBs. The value of σ was determined experimentally where acceptable IC curves without noise were generated. The effect of the filter on the raw IC curve of an LMO cell can be seen in Fig. 6.

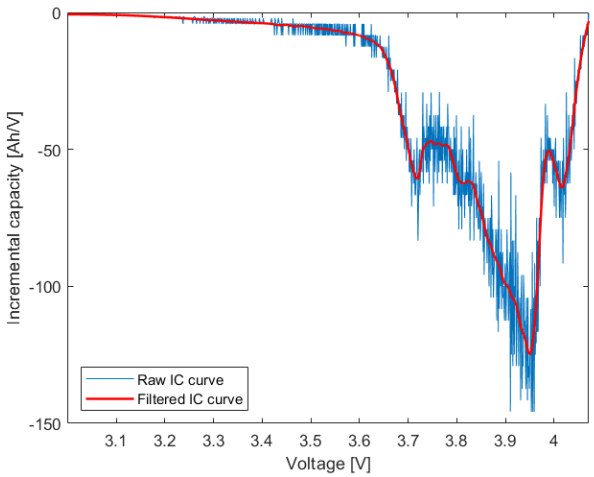

Fig. 6: Raw IC curve and filtered IC curve of LMO cell.

B. Influence of Discharge Current on IC Curves

Fast measurements are most often more favourable than slow measurements. Because of this, it would be best to perform ICA with a discharge current as large as possible. The IC curves of an LMO module with 8 cells in series with discharges 0.25C, 0.5C, and 0.75C can be seen in Fig. 7. There is a clear shift to lower voltages. This shift is not necessarily bad for measurement results since it only offsets the IC curve to the left and does not impair comparisons between IC curves. The major downsides of higher discharge currents are the increased noise present in the IC curve and the reduction in the rightmost peak. The extra noise and new smaller peaks arising in between the leftmost and middle peaks can make it harder to distinguish more subtle characteristics that are present in this region. This could be partially solved by filtering more harshly using the Gaussian filter but that risks information being lost in the process. The reduction in the rightmost peak is the most detrimental to the IC curve since this peak contains much information about the presence of LLI which is one of the major degradation modes. At a discharge current of 0.75C, there is almost no distinguishable peak left past the middle peak and is thus unusable for ICA. All measurements from this point forward will be performed with a discharge current of 0.25C.

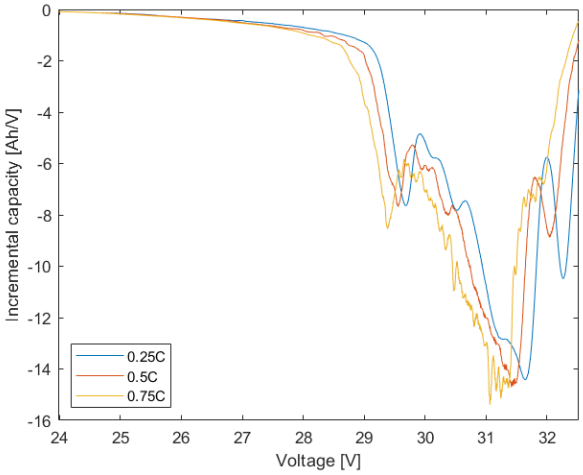

Fig. 7: IC curves of LMO module for different discharge currents.

C. Influence of Individual Cells on Module IC Curve

Since cells in series share the same current the difference in ΔQ of all cells for a given ΔV of the module voltage will be equal. $\Delta Q_{module} = \Delta Q_1 = ... = \Delta Q_n$. When all cells inside a module have aged equally their voltages will be equal at any point during the charge-discharge cycle. If this is the case the module voltage can be expressed as the sum of all cell voltages. $V_{module} = \sum_{i=1}^{n} V_i = n \cdot V$, where n is the amount of cells in series, V_i is the voltage of cell i and V is the voltage that all cells share. When expressing the module IC values in cell voltages and capacities it becomes clear that the IC values on module level are n times smaller than on cell level. This property can be seen in Equation 4. For a good comparison

between IC curves on module level and cell level the module level IC curves should be scaled by a factor n. When IC curves of cells are compared with IC curves of modules, the modules are scaled accordingly. IC curves which contain just modules will be analyzed unscaled.

$$\frac{\Delta Q_{module}}{\Delta V_{module}} = \frac{1}{n} \cdot \frac{\Delta Q_{cell}}{V_{cell}} \tag{4}$$

ICA was performed on individual cells of both the LMO and NMC and on modules of 8 LMO cells and 6 NMC cells in series. First, the LMO cells and module will be discussed. Before analyzing and comparing IC curves it is important to know which cell is the weakest considering only capacity fade. Capacity can easily be measured simultaneously with IC measurements since a CC discharge is performed and the measurement time is known. The capacity of the individual cells in the LMO module can be seen in the bar graph in Fig. 8.

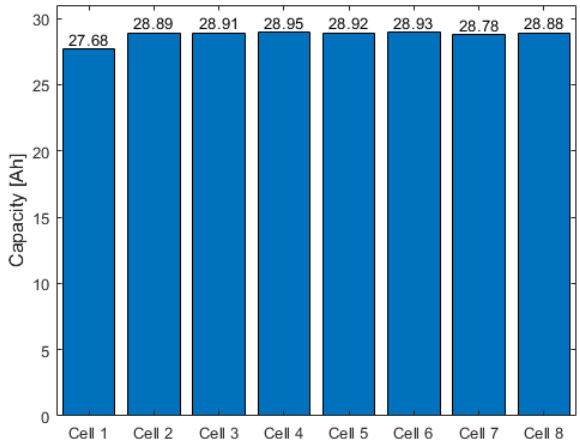

Fig. 8: Capacities of individual cells in LMO module.

1) Cell Level LMO: Cell 1 is the weakest since it has the lowest capacity of all cells and will be compared with the rest of the cells which all have similar capacities. The IC curves of all cells and the IC curve of the module can be seen in Fig. 9.

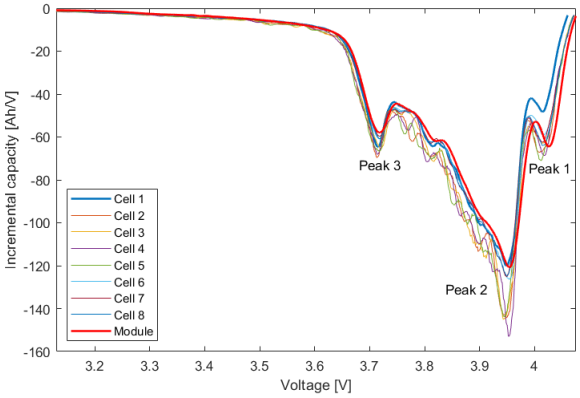

Fig. 9: IC curves of LMO cells and module.

The LMO IC curve has a characteristic IC curve that is quite similar to the LFP IC curve. The LMO also has three distinct peaks which will be referred to from left to right as peaks **3**, **2**, and **1**. the weakest cell has the IC curve with the lowest amplitude for peaks **1** and **2**. Peak **1** is most affected by ageing. The weakest cell has a magnitude that is 32% less than the largest peak **1**. This indicates that the weakest cell has experienced significantly more LLI than the other cells. The weakest cell also has a significantly lower magnitude of peak **2** which is around 21% lower than the largest peak **2**. A close-up of each peak in Fig. 9 can be found in the appendix in Fig. 17. The weakest cell also lies lower in the slope between peaks **2** and **3**. This decrease in overall amplitude indicates that LAM_{NE} has affected the weakest cell more than the other cells. The significant decrease in peak **2** indicates that LLI has occurred to such an extent that peak **1** is depleted and capacity is being lost from underneath peak **2**. The IC curve of the weakest cell has not shifted to the right compared to other cells indicating that the weakest has not experienced more ORI.

When looking at the IC curves of individual LMO cells it is visible that cells whose IC curves indicate less ageing (larger peaks **2** and **3**) have several smaller intermittent peaks in the slope between peaks **2** and **3**. The absence or reduction of intermittent peaks indicates that LLI and/or LAM_{NE} has occurred.

Surprisingly the weakest cell does not have the lowest peak **3**. The second, third, and fourth most aged cells according to the IC curves have the lowest magnitude of peak **3**. The weakest cell has a magnitude of peak **3** between the maximum and minimum values of all IC curves. This could be the result of one or multiple degradation mechanisms increasing peak **3** after a certain amount of ageing. It seems that in earlier stages of ageing peak **3** decreases but eventually starts increasing. This shifting from decreasing to increasing requires further research in the form of a lifetime analysis which tracks peak **3** evolution during ageing. Since lithium plating is known to cause IC peaks to increase this effect could be caused by lithium plating. Especially since lithium plating mostly happens later in the lifetime of LIBs than LLI or LAM and is self-accelerating.

2) Module Level LMO: One of the first things that are noticeable about the module IC curve is that it lies more to the right than any individual IC curve. This is especially visible in the rightmost part of the curve. This shift to the right is quite logical considering the effect ORI has on the IC curve. Since the resistance of multiple cells in series is always bigger than the resistance of an individual cell this will result in an apparent ORI in the IC curve of the module compared to individual cells.

When looking at the peaks of the module IC curve interesting behaviour can be seen. Peak **2** closely follows the weakest cell in the module. The difference in magnitude of peak **2** between the IC curves of the module and the weakest cell is only 0.6Ah/V which is a 0.5% difference. This indicates that the weakest cell in the module most strongly influences the magnitude of peak **2**. If this is consistent with more strongly and weaker differing SOHs between individual cells

module level ICA could determine the peak **2** magnitude of the weakest cell accurately. This property can prove valuable for fast SOH estimations on module level but requires further research.

The module IC curve follows the 4 weakest cells in the slope between peaks **2** and **3**. There are fewer intermittent peaks in the module IC curve and those that are present are in the same relative location as those of the weakest cells. This indicates that the intermittent peaks that are visible for the stronger cells contribute little to the module IC curve. The number of intermittent peaks and their magnitude can thus also provide insight into the weakest cells.

The magnitude of peak **1** in the module IC curve is closely correlated to the mean magnitude of its individual cells. The magnitude of peak **1** of the module only deviates 2.5% from the mean magnitude of its individual cells. The valley between peaks **1** and **2** of the module was also evaluated in the same manner and deviated 3% from the mean of its individual cells. Peak **1** of an LMO module IC curve can thus predict how much LLI has affected the cells on average.

Peak **3** also shows interesting behaviour on module level. Peak **3** of the module IC curve has a lower magnitude than any individual cell. This could indicate that ORI influences peak **3** since the module has a higher internal resistance than any individual cell. This does not rule out the speculated reduction and eventual growth of peak **3**. As stated before more research about peak **3** over the entire LIB lifetime is required.

3) Cell Level NMC: Just like the LMO cells, the first thing to look at to see which cell is the weakest is capacity fade. The capacities of each NMC cell in a module of 6 cells in series can be seen in Fig. 10. Cell 2 and cell 6 are the weakest cells since they have experienced the most capacity fade. Cells 1, 3, and 4 are the strongest cells and all have similar capacitances. Cell 5 has aged slightly more than the strongest cells. It is important to note that these cells are only slightly aged since the weakest cell still has 95% of the lowest typical capacity of 2.75Ah according to the datasheet.

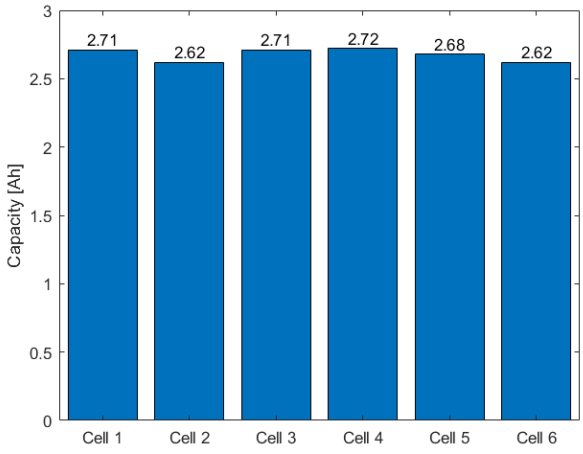

Fig. 10: Capacities of individual cells in NMC module.

The IC curves of all cells and module can be seen in Fig. 11. The characteristic peaks of the NMC IC curves are unique and do not resemble that of LFP or LMO IC curves. Four distinct peaks can be seen which will be referred to as peaks **4** to **1** from left to right.

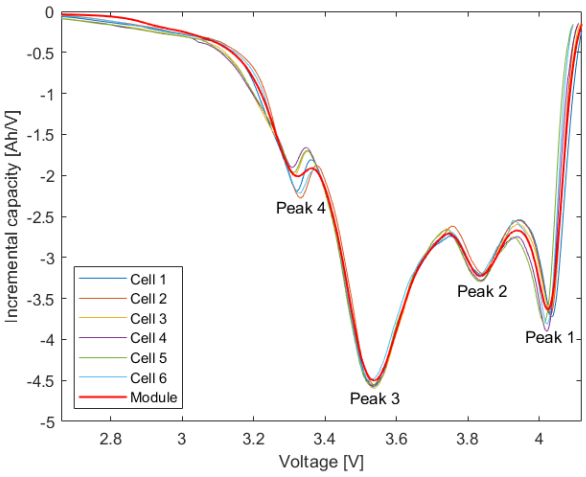

Fig. 11: IC curves of NMC cells and module.

It is noticeable that peaks **2** and **3** have similar magnitudes for all cells. These peaks are thus less affected by ageing in the early lifetime of NMC LIBs. As the cells age further these peaks are expected to decrease as capacity fade increases. This is because the weakest cells are among the lowest in magnitude of peaks **2** and **3**. The IC curves of the weakest cells do not shift uniformly or semi-uniformly to the right so it can not be distinguished which cell has experienced the most ORI.

Peak **1** shows unexpected behaviour. There is no distinct pattern between ageing and peak **1** evolution that can be distinguished on a small ageing scale. The weakest cell does not have the lowest or highest peak **1** magnitude. The strongest cells also do not show the same behaviour. The highest magnitude and lowest magnitude of peak **1** both correspond to one of the strongest cells which have aged equally. There is also no pattern discernible in the horizontal peak location. The behaviour of this peak is most likely caused by measurement errors which will be discussed later on.

Peak **4** evolution does show a significant response to ageing. It is visible that peak **4** is the largest for the weakest cells and shifts to higher voltages. As stated before lithium plating is known to cause IC peaks to emerge and grow. This shift to the right could also be a characteristic of lithium plating in NMC LIBs but could also be caused by sensitivity to ORI in this region.

4) Module Level NMC: The influence of individual cells on the NMC module IC curve is unlike that of LMO modules. The IC curve of the NMC module correlates closely to the mean of all individual cells. The IC curve of the module plotted with the mean of all individual cells can be seen in Fig. 12. In the region between 3.25-4.05V, the module IC curve deviation from the mean IC curve is less than 3%. All peaks lie in this region. In the lower and higher voltage regions the percentual deviation is quite large since the IC curve has low values or high slopes in these regions.

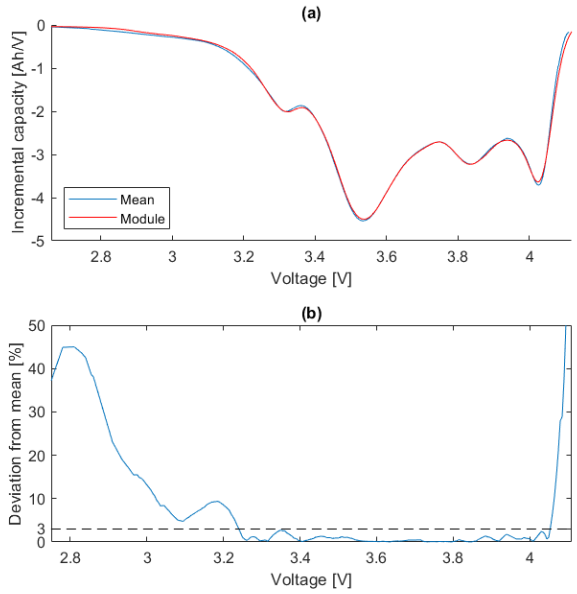

Fig. 12: IC curves of module and mean of all cells (a). Deviation of module IC curve from mean of individual cells (b).

D. Module Comparison

1) LMO Modules: The IC curves of four modules of 8 LMO cells in series were measured. The capacities of each module can be seen in Fig. 13. Module 4 has experienced the most capacity fade and is thus the weakest module. Module 1 is the strongest module. Modules 2 and 3 have aged slightly more than the strongest module.

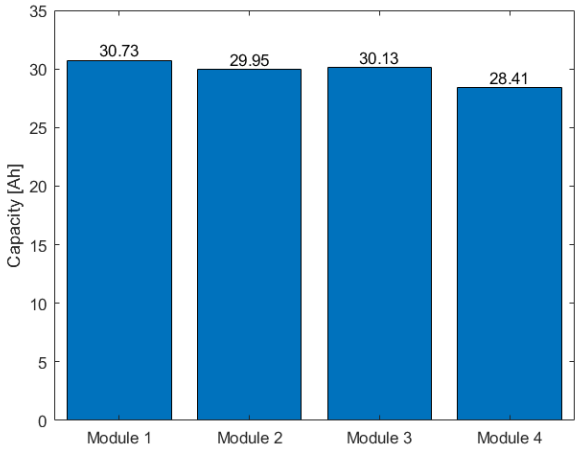

Fig. 13: Capacities of LMO modules.

The IC curves of the four LMO modules can be seen in Fig. 14. As expected the weakest module has the lowest peak **1**. The weakest module has thus experienced more LLI than the other modules. As expected the slope between peaks **2** and **3** also shows less prominent intermittent peaks for the weaker cells. This can be seen more clearly in Fig. 20 in the appendix. It is also visible which modules have experienced the most ORI since the IC curves of modules 2 and 3 are shifted to higher voltages.

Peaks **2** and **3** show interesting behaviour. It is expected that the weakest module would have the lowest peak **2**. However, the weakest module has the highest peak **2**. Peak **2** on module level correlates with peak **2** of the weakest cell inside. This could mean that there are individual cells inside the stronger modules that have smaller magnitudes for peak **2** than the weakest cell in the weakest module. Another cause for this could be that the stronger modules have experienced more LAM_{NE} and less LLI. This would explain the relatively high magnitudes of peak **1** while peak **2** is lower than expected.

Peak **3** also shows interesting behaviour on module level. The strongest module should have the highest peak **3**. However, only the weakest module has a lower magnitude of peak **3** than the strongest module. The reason for this could be the previously speculated causes for the behaviour of peak **3**. The lower magnitude of peak **3** of the strongest module could be caused by ORI since it was speculated that ORI causes a decrease in peak **3**. However, it was already found that weaker modules have experienced the most ORI so this explanation is flawed. The other reason for this behaviour could be the growth of peak **3**. It was speculated that lithium plating can cause peak **3** to grow. If the modules with larger peak **3** magnitude have indeed experienced more lithium plating than the strongest module this can be the cause.

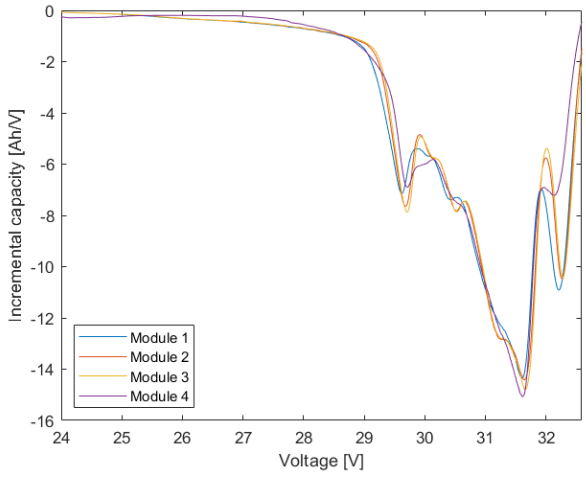

Fig. 14: IC curves of LMO modules.

2) NMC Modules: In Fig. 15 the IC curves of an aged and unaged NMC module with 6 cells in series can be found. The first things that can be seen and are as expected are the growth and shift of peak **4** and a decrease in peaks **3** and **2** with peak **3** decreasing the most.

The valley in between peaks **2** and **3** shows a clear reduction in magnitude of the aged module. This could be an indicator of LLI since a substantial amount of area underneath the IC curve and thus capacity is lost in this region. There is also a shift to the right of peak **2** which could be caused by ORI.

Another noticeable aspect of the IC curves in Fig. 15 is that the aged module has a higher magnitude of peak **1** than

the unaged module. Just like on cell level there is no pattern which can be distinguished in peak **1** evolution during ageing. This is once again most likely caused by measurement errors which will be discussed in the following section.

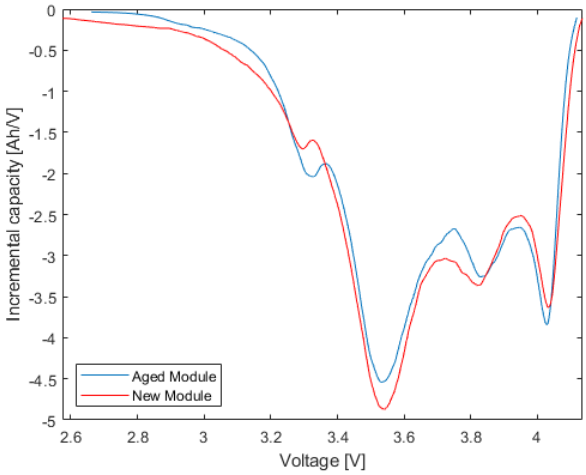

Fig. 15: IC curves of NMC modules.

E. Measurement Errors

LIB measurements are very sensitive to changes in initial conditions. For IC measurements it is important that the cell has the exact SOC at the start of every measurement and that it has been idle for a sufficient or same amount of time after charging. Temperature also influences the IC curve but as stated before all measurements were performed at 23C°. To ensure a constant initial SOC across measurements a power supply which cuts off the LIB when the charging current has dropped below a certain value in the CV charging stage can be used. Another even more sophisticated method would be to monitor the precise charge that has entered the LIB during charging using a coulomb counter which can accurately measure SOC. Unfortunately, this equipment was unavailable so it was not possible to ensure a constant initial SOC across all IC measurements. Due to time constraints, the amount of time between charging and measuring was inconsistent and sometimes insufficient. As can be seen in Fig. 16 the deviation between measurements is mostly present in the higher voltage range. This is logical since the CV charging stage is the final stage of battery charging and happens at the maximum voltage of the LIB. If the charging process of one measurement is cut off earlier there will be less capacity present in the higher voltage range resulting in a lower magnitude of peak **1**. Other peaks are less affected since the lower voltage ranges are only affected by the CC stage of charging. These deviations between measurements overshadowed peak **1** evolution in the NMC cells and modules. For all other measurements, the ageing processes either had a stronger influence on the IC curve than the measurement deviations or the measurement deviations were insignificant.

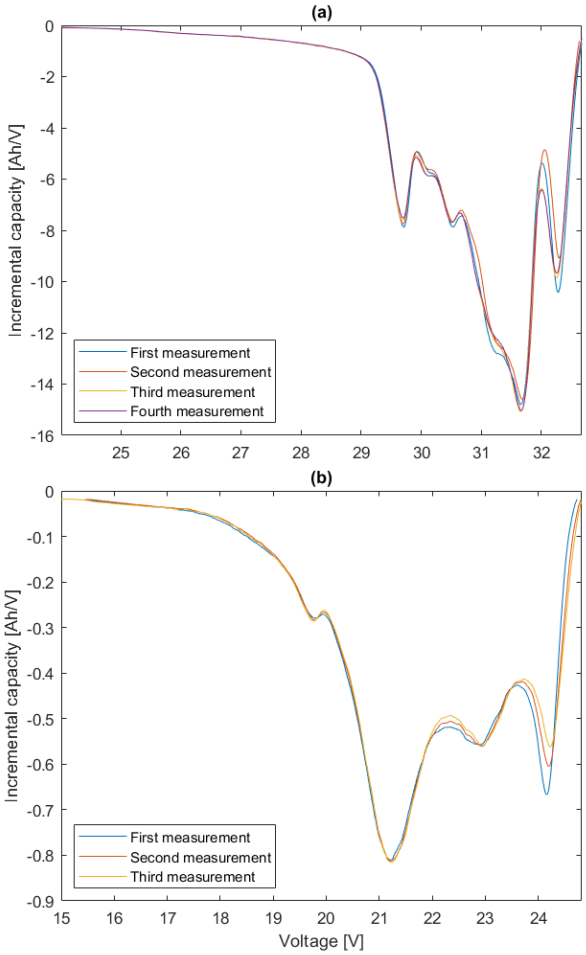

Fig. 16: Different IC measurements of same LMO module (a). Different IC measurements of same NMC module (b).

IV. Conclusion

In this paper, the application of ICA on module level was researched. ICA was performed on individual cells and multiple modules with LMO and NMC battery chemistries. Both battery chemistries had different IC curves which responded differently to ageing. The influence of individual IC curves on the module IC curve was also different for both battery chemistries. The most significant findings are the correlation between LMO module and cell peaks in the IC curves and the correlation between IC curves of NMC modules and the mean of its cells. It was found that LMO modules have a peak in the IC curve that is most strongly influenced by its weakest cell and thus almost exactly follows the IC curve of the weakest cell at this peak. The deviation between the weakest cell and module was only 0.5% for this IC peak. This is a promising result for further research as parameters of the weakest cell can be measured on module level. It was also found that NMC module IC curves follow the mean of the individual cell IC curves. NMC module IC curves deviation from the mean of its cells stayed below 3% in the region of the curve in which all IC peaks lie. This property can be used to investigate average degradation of NMC LIB modules. It can thus be concluded

that ICA is a useful battery analysis method for module level LIBs.

The effects ageing has on IC curves of these battery chemistries are summarized in the following list. These effects were used to compare modules of these battery chemistries.

- LMO Cell
  - LLI causes peak **1** reduction.
  - LAM_{NE} causes reduction across entire IC curve.
  - ORI causes shifting to higher voltages.
  - Reduction in magnitude and number of intermittent peaks between peaks **2** and **3**.
  - Initial reduction in peak **3** but eventual growth after sufficient ageing (possibly caused by lithium plating).
- LMO Module
  - Shifting to higher voltages caused by apparent ORI compared to individual cells.
  - Peak **2** magnitude correlates with peak **2** magnitude of the weakest cell inside the module.
  - Intermittent peaks between peaks **2** and **3** correlate with intermittent peaks of weakest cells inside the module.
  - Peak **1** magnitude correlates with the mean of peak **1** magnitude of all cells inside the module.
  - Peak **3** magnitude is lower than peak **3** magnitudes of any singular cell (possible dependence of ORI on peak **3**).
- NMC Cell
  - Peak **2** and **3** stay constant under small ageing variation.
  - Peak **4** is more sensitive to ageing and grows and shifts to higher voltages (possibly caused by lithium plating and ORI).
  - Peak **1** was too harshly influenced by measurement error for analysis.
- NMC Module
  - Module IC curve correlates with mean of individual IC curves.
  - Peak **4** behaves as peak **4** of an individual cell.
  - Reduction of peaks **2** and **3** with peak **3** experiencing the most reduction.
  - Large loss of area underneath curve at the valley between peaks **2** and **3** (possibly caused by LLI).
  - Peak **1** was too harshly influenced by measurement error for analysis.

V. Future Work

This paper discussed the effect that ageing has on the IC curves of LMO and NMC batteries on cell level and module level. Some speculations were made that require further research in the form of a lifetime analysis of the IC curves. Peak **3** of the LMO LIBs showed unexpected behaviour which would be interesting to track over the entire lifetime of LMO cells and modules. It would also be interesting to investigate if the property of peak **2** of LMO modules having the same magnitude as peak **2** of their weakest cell is valid across the entire lifetime. The intermittent peaks between peaks **2** and **3** in LMO IC curves are also a little researched subject which could prove useful for SOH estimations. For the NMC cells, a comparison of the aged and unaged individual cells would be useful to investigate the cell level IC curve evolution on a larger ageing scale. Unfortunately, due to time constraints, this was not possible to investigate. The correlation between the NMC module IC curve and the mean of all its individual cells can also prove useful for SOH estimations, if this is valid across the entire lifetime. Finally in order to analyse peak **1** of the NMC cells and modules the measurement setup should be improved. A reliable method of charging the LIBs and a consistent and sufficient idling period should be implemented in order to decrease measurement deviation. As stated before this can be done by using a power supply with a cut-off current function or a coulomb counter.

VI. References

[1] Micah S. Ziegler and Jessika E. Trancik. "Re-examining rates of lithium-ion battery technology improvement and cost decline". In: *Energy Environ. Sci.* 14 (4 2021), pp. 1635–1651. URL: http://dx.doi.org/10.1039/D0EE02681F.

[2] International Energy Agency (IEA). *Global EV outlook 2020 entering the decade of electric drive?* 2020. URL: https://www.iea.org/reports/global-ev-outlook-2020.

[3] M. R. Palacín and A. de Guibert. "Why do batteries fail?" In: *Science* 351.6273 (2016), p. 1253292. URL: https://www.science.org/doi/abs/10.1126/science.1253292.

[4] Linda Gaines. "Lithium-ion battery recycling processes: Research towards a sustainable course". In: *Sustainable Materials and Technologies* 17 (2018), e00068. URL: https://www.sciencedirect.com/science/article/pii/S2214993718300629.

[5] Bruce Dunn, Haresh Kamath, and Jean-Marie Tarascon. "Electrical Energy Storage for the Grid: A Battery of Choices". In: *Science* 334.6058 (2011), pp. 928–935. URL: https://www.science.org/doi/abs/10.1126/science.1212741.

[6] Juner Zhu et al. "End-of-life or second-life options for retired electric vehicle batteries". In: *Cell Reports Physical Science* 2.8 (2021). URL: https://www.sciencedirect.com/science/article/pii/S2666386421002484.

[7] J. Vetter et al. "Ageing mechanisms in lithium-ion batteries". In: *Journal of Power Sources* 147.1 (2005), pp. 269–281. URL: https://www.sciencedirect.com/science/article/pii/S0378775305000832.

[8] Satu Kristiina Heiskanen, Jongjung Kim, and Brett L. Lucht. "Generation and Evolution of the Solid Electrolyte Interphase of Lithium-Ion Batteries". In: *Joule* 3.10 (2019), pp. 2322–2333. URL: https://www.sciencedirect.com/science/article/pii/S2542435119304210.

[9] Roman Imhof and Petr Novák. “In Situ Investigation of the Electrochemical Reduction of Carbonate Electrolyte Solutions at Graphite Electrodes”. In: *Journal of The Electrochemical Society* 145.4 (1998), pp. 1081–1087. URL: https://doi.org/10.1149/1.1838420.

[10] Thomas Waldmann, Björn-Ingo Hogg, and Margret Wohlfahrt-Mehrens. “Li plating as unwanted side reaction in commercial Li-ion cells – A review”. In: *Journal of Power Sources* 384 (2018), pp. 107–124. URL: https://www.sciencedirect.com/science/article/pii/S0378775318301848.

[11] Qianqian Liu et al. “Understanding undesirable anode lithium plating issues in lithium-ion batteries”. In: *RSC Adv.* 6 (91 2016), pp. 88683–88700. URL: http://dx.doi.org/10.1039/C6RA19482F.

[12] Uwe Westerhoff et al. “Analysis of Lithium-Ion Battery Models Based on Electrochemical Impedance Spectroscopy”. In: *Energy Technology* 4.12 (2016), pp. 1620–1630. URL: https://onlinelibrary.wiley.com/doi/abs/10.1002/ente.201600154.

[13] Nina Harting et al. “Nonlinear Frequency Response Analysis (NFRA) of Lithium-Ion Batteries”. In: *Electrochimica Acta* 248 (2017), pp. 133–139. URL: https://www.sciencedirect.com/science/article/pii/S0013468617307934.

[14] Jiangtao He et al. “State-of-Health Estimation of Lithium-Ion Batteries Using Incremental Capacity Analysis Based on Voltage–Capacity Model”. In: *IEEE Transactions on Transportation Electrification* 6.2 (2020), pp. 417–426.

[15] M. Berecibar et al. “Degradation Mechanisms Detection for HP and HE NMC Cells Based on Incremental Capacity Curves”. In: *2016 IEEE Vehicle Power and Propulsion Conference (VPPC)*. 2016, pp. 1–5.

[16] Yi Li et al. “A quick on-line state of health estimation method for Li-ion battery with incremental capacity curves processed by Gaussian filter”. In: *Journal of Power Sources* 373 (2018), pp. 40–53. URL: https://www.sciencedirect.com/science/article/pii/S0378775317314532.

[17] Daniel-Ioan Stroe and Erik Schaltz. “Lithium-Ion Battery State-of-Health Estimation Using the Incremental Capacity Analysis Technique”. In: *IEEE Transactions on Industry Applications* 56.1 (2020), pp. 678–685.

[18] David Anseán et al. “Lithium-Ion Battery Degradation Indicators Via Incremental Capacity Analysis”. In: *IEEE Transactions on Industry Applications* 55.3 (2019), pp. 2992–3002.

[19] Elie Riviere et al. “Innovative Incremental Capacity Analysis Implementation for C/LiFePO4 Cell State-of-Health Estimation in Electrical Vehicles”. In: *Batteries* 5.2 (2019). URL: https://www.mdpi.com/2313-0105/5/2/37.

[20] Amelie Krupp et al. “Incremental Capacity Analysis as a State of Health Estimation Method for Lithium-Ion Battery Modules with Series-Connected Cells”. In: *Batteries* 7.1 (2021). URL: https://www.mdpi.com/2313-0105/7/1/2.

[21] Akram Eddahech, Olivier Briat, and Jean-Michel Vinassa. “Performance comparison of four lithium–ion battery technologies under calendar aging”. In: *Energy* 84 (2015), pp. 542–550. URL: https://www.sciencedirect.com/science/article/pii/S0360544215003138.

[22] Zengkai Wang et al. “State of health estimation of lithium-ion batteries based on the constant voltage charging curve”. In: *Energy* 167 (2019), pp. 661–669. URL: https://www.sciencedirect.com/science/article/pii/S0360544218322126.

[23] Chroma. *6310A Operation Programming Manual 202103*. Tech. rep. Mar. 2021. URL: https://www.chromausa.com/document-library/manuals-6310a-series/.

[24] Xiaoyu Li et al. “State of health estimation for Li-Ion battery using incremental capacity analysis and Gaussian process regression”. In: *Energy* 190 (2020), p. 116467. URL: https://www.sciencedirect.com/science/article/pii/S0360544219321620.

VII. Appendix

```
% v - Voltage measurement data
% Q - Capacity measurement data
% dQdv - IC values
% dv - Voltages corresponding to IC values

dQdv = [];
dv = [];

temp = 1;
prevV = v(1);

for i = 1:length(v)
    if (v(i) < prevV)
        dQdv(end+1) = (Q(i)-Q(temp))/(v(i)-v(temp));
        dv(end+1) = v(i);
        prevV = v(i);
        temp = i;
    end
end
```

MATLAB code for computing IC curves

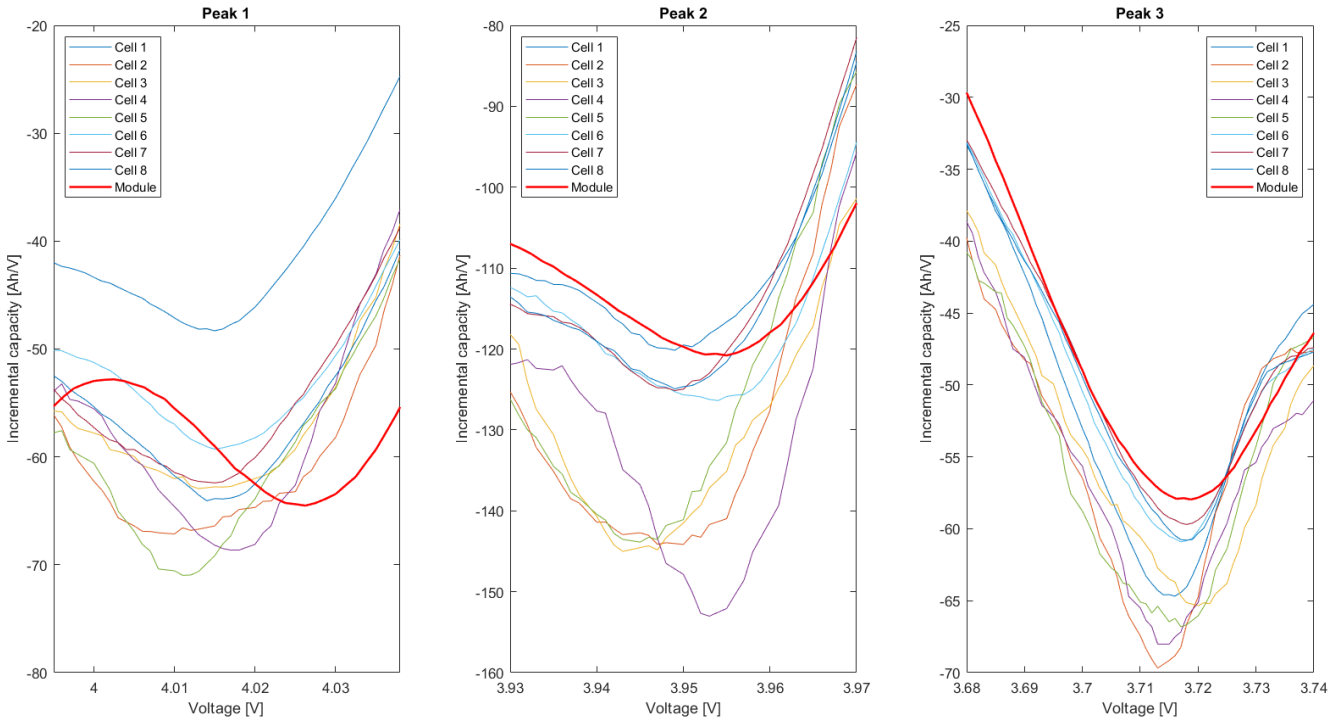

Fig. 17: Close-ups of IC peaks of LMO cells and module

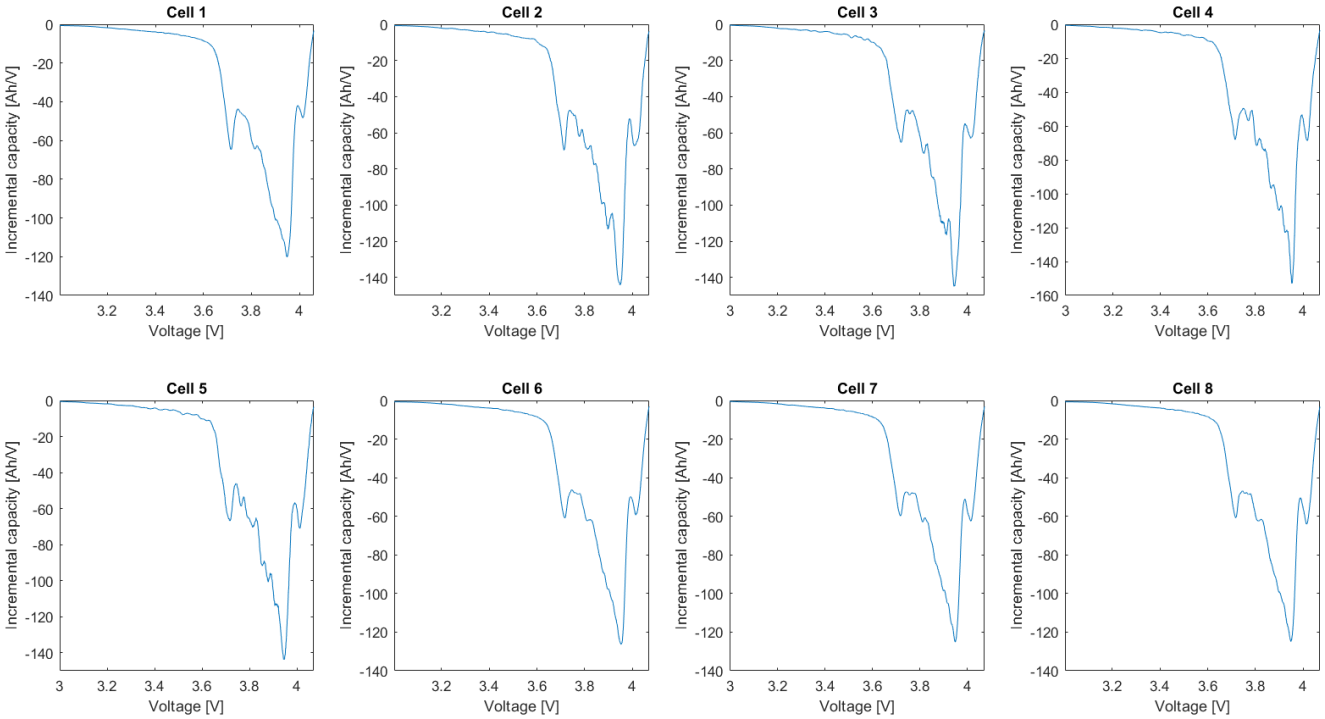

Fig. 18: IC curves of LMO cells plotted separately

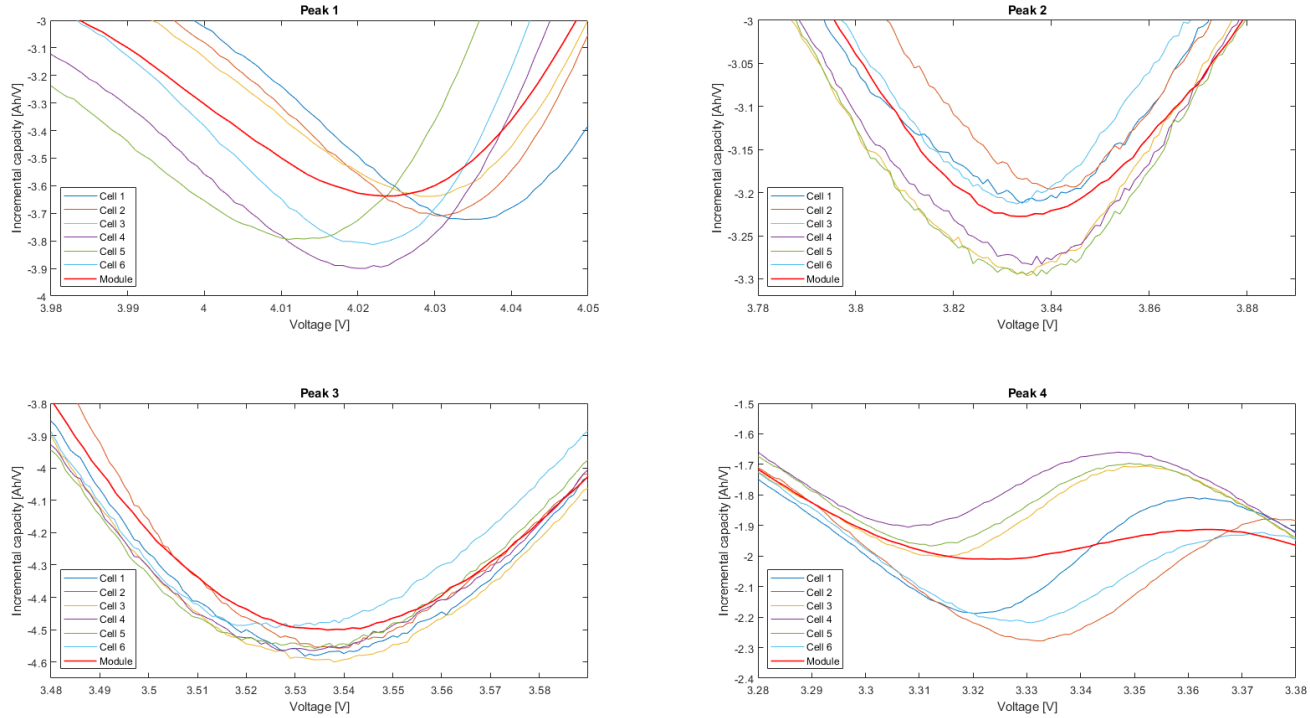

Fig. 19: Close-ups of IC peaks of NMC cells and module

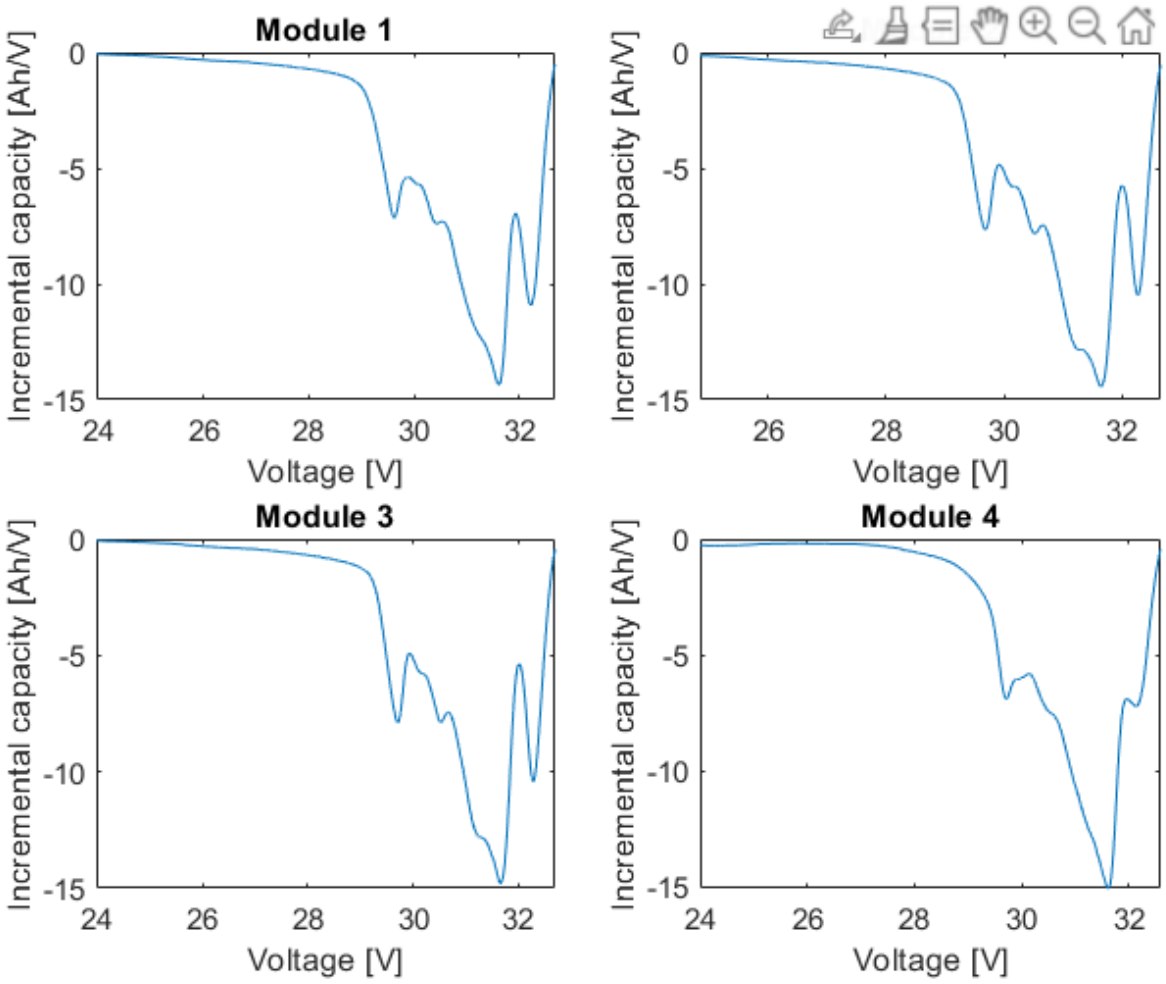

Fig. 20: IC curves of LMO modules plotted separately